

## 2-D Algorithm for Removing STIS Echelle Scattered Light

Jeff Valenti, Ivo Busko, and Jessica Kim Quijano

Space Telescope Science Institute, 3700 San Martin Drive, Baltimore, MD 21218

Don Lindler

Advanced Computer Concepts, Inc.

Chuck Bowers

Goddard Space Flight Center, Greenbelt, MD 20771

**Abstract.** We provide excerpts from *Instrument Science Report STIS 2002-01* (Valenti et al. 2002), which describes in more detail a 2-D algorithm for removing scattered light from STIS echelle spectra.

### 1. Introduction

Ideally, a spectrograph should yield a one-to-one mapping between detector pixel and monochromatic source intensity. In practice, background, scattered light, and finite resolution contaminate the monochromatic signal in each pixel. Background subtraction and scattered light removal typically precede spectral extraction. Bias and dark subtraction removes the component of background that is independent of exposure level, leaving only the source spectrum and a component due to scattered light. For echelle spectrographs, 1-D linear interpolation of the minimum intensity between echelle orders provides a simple model of the scattered light beneath each order. Originally, this basic scattered light model was the only choice in the IRAF task `x1d` (McGrath et al. 1999), which is often used to extract echelle spectra obtained with the Space Telescope Imaging Spectrograph (STIS). Beginning with CALSTIS version 2.9 (installed in the archive pipeline on 2000 Dec 21 and released as part of STSDAS version 2.3 on 2001 June 12), `x1d` also includes a new 2-D scattered light model (*algorithm = sc2d*) that supplements the original 1-D model (*algorithm = unweighted*). The *sc2d* algorithm was developed by Lindler & Bowers (2001), implemented in CALSTIS by Busko, and tested by Valenti.

Several authors have suggested simple enhancements of the basic 1-D algorithm. For example, Howk & Sembach (2000) inferred the background beneath each order by fitting 1-D polynomials to an extended region around the minima between echelle orders. Alternatively, scattered light may be decomposed into a local 1-D component that scales with counts detected in the two immediately adjacent orders and a global 2-D polynomial component (e.g., Gehren & Ponz 1986). The formalism developed to interpret echelle data from the Goddard High-Resolution Spectrograph includes components that scale with total counts in an order and counts detected in each extracted wavelength bin (Cardelli et al. 1993). These 1-D components correspond to scatter by the echelle and the cross-disperser, respectively. In contrast to the models described above, the *sc2d* algorithm iteratively builds an empirical 2-D description of scattered light from 1-D extracted spectra and known scattering properties of the telescope and spectrograph.

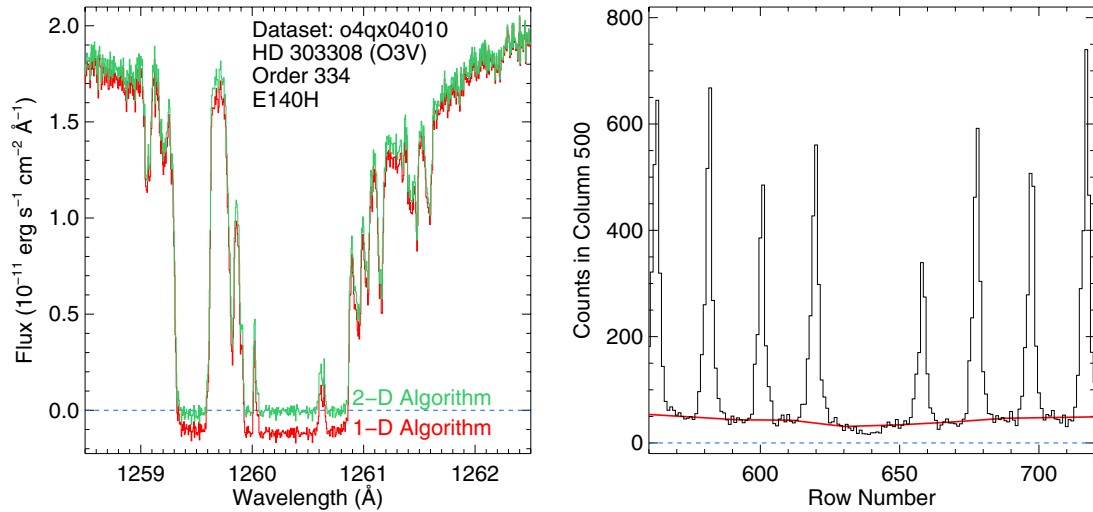


Figure 1. *Left*: These interstellar absorption lines should have zero flux in the line cores, but extraction with a 1-D scattered light model yields negative fluxes. *Right*: In this cut across echelle orders, the deep absorption line in the order at row 640 drops below the 1-D scattered light model (smooth horizontal line).

## 2. Empirical Motivation

Development of a background subtraction algorithm (Lindler & Bowers 2001) with a 2-D scattered light model was motivated by unrealistic negative fluxes in saturated cores of interstellar absorption lines punctuating spectra of continuum sources. Figure 1a demonstrates the problem with extracted spectra obtained by subtracting either 1-D or 2-D estimates of the scattered light background. With the traditional 1-D background subtraction algorithm, the saturated line core is systematically below zero by  $9.0 \pm 0.4\%$  of the neighboring continuum flux. This must be an artifact of inadequate background subtraction. With the new 2-D scattered light model described here, the line core is only  $1.0 \pm 0.4\%$  below zero, indicating significant improvement.

Figure 1b presents a cut at column 500 through the subimage in Figure 2a. Echelle orders 330–338 are spaced nearly uniformly, except that order 334 is missing because of the strong interstellar line extracted in Figure 1a. The unweighted algorithm in `x1d` estimates the background beneath each order by linearly interpolating the mean interorder light along columns. Order 334 (near row 640) is systematically below the 1-D background estimate (smooth horizontal line), indicating the need for a better background estimate.

Figure 2a shows a portion of a cross-dispersed echelle spectrum obtained in the FUV with the STIS E140H grating. The continuum of HD 303308 (black horizontal bands) is cut by interstellar absorption lines (white gaps) which should have zero signal in the final extracted spectrum. The image in Figure 2a has been clipped at 6% of the peak to highlight the behavior of the background. Note that absorption line cores are fainter (whiter) than the “background” between echelle orders. In this case, linear interpolation of interorder light along columns does not provide a good estimate of the background beneath an order.

Lindler & Bowers (2001) developed a 2-D algorithm which provides a better estimate of the background everywhere on the detector. Figure 2b shows the resulting 2-D background estimate for the subimage shown in the left panel. The region around the strongest interstellar line complex is highlighted (dashed box) in both images. The background between orders is brighter (blacker) than the general background beneath each order, which in turn is higher than the faint background (white patches) beneath strong absorption lines.

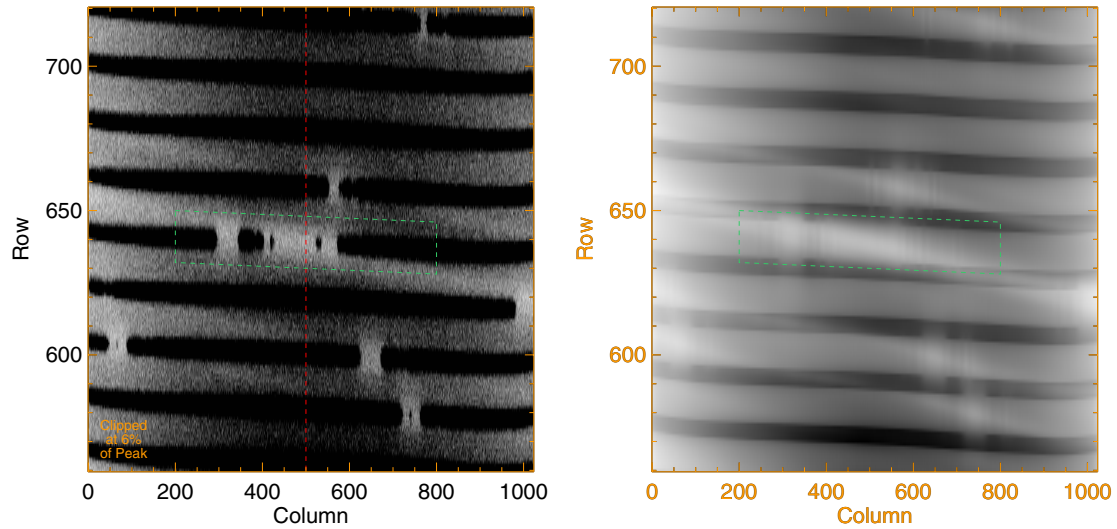


Figure 2. *Left:* Counts in deep absorption lines are below (less dark) than the background between orders. A vertical line indicates the cut used in Figure 1. *Right:* The 2-D scattered light model is lower (less dark) in the cores of deep absorption lines. A rectangle outlines the same regions as in the left panel.

### 3. Algorithm

In the Lindler and Bowers (2001) algorithm, a flat-fielded image is fitted with a 2-D model constructed in each iteration by folding the best current estimate of the extracted spectrum through a semi-empirical simulation of STIS optical properties. For STIS data, self-consistency between the model image and the extracted spectrum is achieved after three iterations. A 2-D scattered light model is then constructed considering only the echelle scatter outside an 11 pixel wide vertical window centered on each order. This 2-D scattered light model is subtracted from the original image, and the final spectrum is obtained using standard 1-D extraction. See Valenti et al. (2002) for details.

Scattered light from the echelle gratings is a significant contribution to STIS scattered light and is the main reason why a 1-D background model does not accurately reflect the scattered light beneath an order. Figure 3a shows echelle scatter functions for three orders of the E140M grating. A majority of the light is concentrated in the central pixel, but integrated light in the wings of the scattering function can be significant. At the shortest wavelengths, 37% of the light is scattered more than 15 pixels from the nominal position. As indicated in the table inset, scattered light increases dramatically at the short wavelength end of the FUV bandpass, presumably because the wavelength of incident light is becoming comparable to the size of irregularities on the reflection grating surface. At visible wavelengths, echelle scatter would be greatly diminished, reducing the need for a 2-D scattered light algorithm.

### 4. STSDAS Implementation

The 2-D algorithm was first implemented by Lindler in IDL, taking advantage of the software and database environment maintained for the STIS Instrument Definition Team. Busko incorporated the algorithm into the existing `x1d` task in the IRAF package STSDAS. The `x1d` implementation is used in the archive pipeline and is supported for general use by the STIS community. Both the IDL and IRAF implementations have tasks named CALSTIS that drive end-to-end processing of STIS data, so an additional descriptor is required to distinguish between the two implementations (e.g., “the `sc2d` algorithm in the `x1d` task” uniquely specifies the IRAF implementation). The `sc2d` algorithm

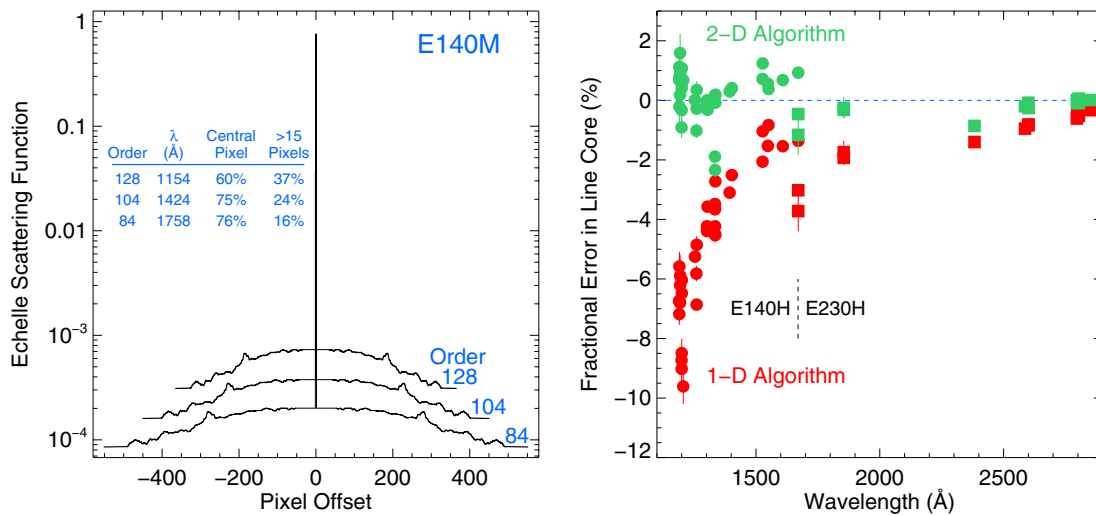


Figure 3. *Left:* Echelle scatter is modelled as a sharp core with broad wings. At short wavelengths, 1/3 of the light is scattered by more than 15 pixels. *Right:* The cores of numerous deep absorption lines yield errors, relative to the local continuum and as a function of wavelength, for 1-D and 2-D models.

in `x1d` first appeared in CALSTIS version 2.9, which was installed in the archive pipeline on 2000 Dec 21 and released as part of STSDAS version 2.3 on 2001 June 12.

The 2-D algorithm requires a component level description of STIS optical properties, which Lindler and Bowers bundled into a variety of reference files. Implementation of the `sc2d` algorithm in `x1d` required the creation of 7 new reference file types, beyond those required for the original unweighted algorithm. Scattered light reference files used by the `sc2d` algorithm in `x1d` have content identical to the original Lindler reference files, but organization and FITS structure have been modified to match STSDAS conventions.

Figure 3b shows measured errors for strong absorption interstellar line cores, as a function of wavelength and echelle grating. Although the four echelle gratings could in principle have significantly different surface roughness, 1-D extraction errors for all the echelle gratings have a similar dependence on wavelength. The factor of four increase in error from 1400 to 1100 Å, despite only a factor of two increase in echelle scatter over the same interval (table inset in Figure 3a), may simply be due to the decrease in order spacing for bluer orders. This same effect could also account for the larger errors in E230H spectra at 1700 Å, relative to E140H spectra.

## References

- Cardelli, J. A., Ebbets, D. C., & Savage, B. D. 1993, *ApJ*, 413, 401  
 Gehren, T. & Ponz, D. 1986, *A&A*, 168, 386  
 Howk, J. C. & Sembach, K. R. 2000, *AJ*, 119, 2481  
 Lindler, D. & Bowers, C. 2001, *BAAS*, 197.1202  
 McGrath, M. A., Busko, I., & Hodge, P. 1999, *Instrument Science Report STIS 1999-03* (Baltimore: STScI)  
 Valenti, J. A., et al. 2002, *Instrument Science Report STIS 2002-01* (Baltimore: STScI)